pH-Sensitive Breathing of Clay within the Polyelectrolyte Matrix

Piyush Chaturbedy,[†] Dinesh Jagadeesan,[†,‡] and Muthusamy Eswaramoorthy[†,*]

[†]Nanomaterials and Catalysis Lab, Chemistry and Physics of Materials Unit, DST Unit on Nanoscience, Jawaharlal Nehru Centre for Advanced Scientific Research, Bangalore-560064, India. [‡]Present address: Lash Miller Chemical Laboratories, University of Toronto, Ontario M6S 3H6, Canada.

ABSTRACT Stimuli-responsive organic—inorganic hybrid spheres were synthesized by coating the colloidal polystyrene spheres with polyelectrolyte-protected aminoclay, Mg phyllo(organo)silicate layers in a layer-by-layer method. The clay layers are sandwiched between the polyelectrolyte layers. The aminoclay swells in water due to protonation of amino groups, and the degree of swelling depends on the pH of the medium. As a result, the hybrid spheres undergo a size change up to 60% as the pH is changed from 9 to 4. The stimuli-responsive property of the hybrid spheres was used for the release of ibuprofen and eosin at different pH.

KEYWORDS: stimuli responsive · microcapsules · layer-by-layer assembly · layered materials · hybrid materials

Advanced futuristic technologies are expected to consist of devices that can operate and even make logical decisions on their own. A successful evolution of such a technology must certainly involve individual components that not only are capable of sensing small changes in their environment but also can respond to such changes. Materials with such abilities are broadly termed smart materials or stimuli-responsive materials.[1−4] Materials that can respond to various types of stimulus such as mechanical stress,[5] temperature,[6,7] pH,[8−12] electric field,[13] magnetic field,[14] redox potentials,[15] light,[16,17] and certain chemicals[18,19] have been synthesized in the past.[18,19] Organic materials such as polyelectrolyte multilayers,[20] block copolymers,[21] phospholipids,[22] and gels[23] possess individual molecular components that can respond to an external stimulus by significantly altering their own physical or chemical properties. On the other hand, inorganic shape-memory alloys,[24] piezoelectric and pyroelectric materials,[25−27] and smart window materials[28] achieve their smartness by virtue of their ability to reversibly alter the crystal structure or lattice volume in response to an external stimulus. Recently, there has been interest in the synthesis of stimuli-responsive composite materials that are made up of organic and inorganic components.[29−36] The composites, besides offering a wider range of options to tune the functionality at the molecular scale (organic component), also provide remarkable robustness (inorganic component).[29] When such systems are tuned to respond to changes in a window of physiologically relevant conditions, many applications in biodiagnosis and controlled drug delivery can be achieved.[2,3] In this report, we describe the synthesis of stimuli-responsive composite spheres composed of organoclay layers protected within the polyelectrolyte matrix. There have been examples in the literature where layered inorganic materials have been used as one of the components of stimuli-responsive material. Brinker et al. reported a reversible change in the interlayer spacing of hybrid layered silicate derived from an azobenzene-bridged silsesquioxane,[37] in response to photophysical stimuli. Nevertheless, the change in the interlayer spacing is restricted by the dimensions allowed by *cis*−*trans* isomerism of the azobenzene moiety. Mann et al. reported the transformation of perforated microspheres of Mg phyllo(hexadecyl)silicates to apple-shaped structures by prolonged swelling in *n*-octane.[38] However, the hydrophobic nature of these materials limits their use in the controlled delivery of hydrophilic drugs/molecules in the physiological environment. Therefore, making hydrophilic layered materials in the form of spheres/capsules that could respond to external stimuli will have an added advantage, as they can be used to encapsulate and control the release of drug molecules within the layers as well as from the core. Though there are very few reports on the synthesis

*Address correspondence to eswar@jncasr.ac.in

Received for review April 6, 2010 and accepted September 27, 2010.

Published online October 7, 2010.
10.1021/nn100700b

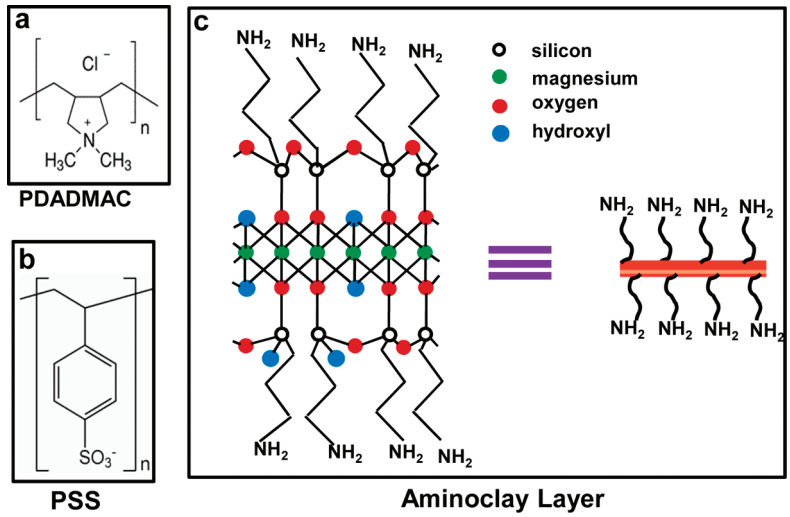

Figure 1. Molecular structure of (a) PDADMAC, (b) PSS, and (c) aminoclay.

of clay hollow spheres, to our knowledge they did not show any stimuli-responsive behavior with respect to chemical or physical environment.[39−41] Here, we have shown a clay, having the ability to swell at different pH, wrapped in a polyelectrolyte matrix could reversibly change the size of the spheres with pH, which has been used in a controlled release of small molecules.

RESULTS AND DISCUSSION

Polystyrene spheres (PS) used in this study were synthesized by standard emulsion polymerization technique.[42] The polyelectrolytes used were poly(diallyldimethylammonium) chloride (PDADMAC) and poly(styrenesulfonate) (PSS) (Figure 1a and b). The aminoclay used in this study is Mg phyllo(organo)silicates having a structure analogous to 2:1 trioctahedral smectites and was synthesized by a chemical method.[43,44] Its structure consists of a central brucite sheet of octahedrally coordinated MgO/OH chains sandwiched between a tetrahedral organosilicate network containing covalently linked propylamine pendant groups with an approximate unit cell composition of $R_8Si_8Mg_6O_{16}(OH)_4$, where R = $CH_2CH_2CH_2NH_2$ (Figure 1c).[44] In water, the clay layers are positively charged over a wide range of pH due to the protonation of the amine groups (Figure 2) (alkylamine $pK_b \approx 3.4$).[45] As a result, the electrostatic repulsion between the protonated clay layers exfoliates the clay and forms a transparent dispersion in water. The extent of protonation of amine groups (and hence the exfoliation) increases with a decrease in pH, which, in turn, increases the charge density on the individual clay layers. The decrease in clay particle size observed in dynamic light scattering (DLS) with a decrease in pH further supports the exfoliation of clay layers due to the increased level of protonation at low pH (Figure 2).

The composite spheres were synthesized by a well-established electrostatic layer-by-layer technique (LbL)[46−50] (Scheme 1). This technique usually involves the sequential adsorption of polyelectrolytes of opposite charges on a charged planar surface or around the colloidal spheres. The method has been successfully applied to generate composite films from nanoparticles,[51] nanotubes and nanowires,[52,53] nanoplates,[54,55] DNA,[56] proteins,[57,58] viruses,[59] lipids,[60] *etc*. This method was further extended to make nano- and microcapsules using sacrificial colloidal spheres as templates.[61−63] In Scheme 1, we describe the experimental protocol to synthesize the stimuli-responsive composite of clay and polyelectrolytes. The as-prepared PS spheres were used as cores around which the polyelectrolytes and clay were sequentially coated. Initially, colloidal PS spheres were coated with PDADMAC as layer 1 followed by the adsorption of PSS as layer 2. The first two coatings of charged polyelectrolytes over PS are essential to facilitate the subsequent adsorption of clay as the third layer. Finally, the clay layer was wrapped with a layer of negatively charged PSS. The as-prepared samples were designated as PSL1, PSL2, PSL3, and PSL4, respectively, depending on the number of layers coated on the PS core. A control sample, PSL4-NC (PSL4-No Clay), was also synthesized wherein the third layer of clay was replaced with a layer of PDADMAC.

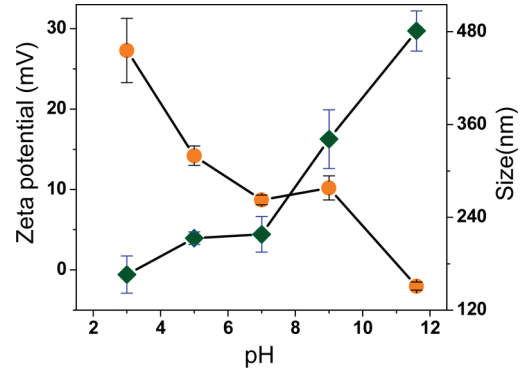

Figure 2. Basic information about aminoclay. Plot of zeta potential of clay vs pH (orange circles) and hydrodynamic diameter of clay particles vs pH (olive diamonds).

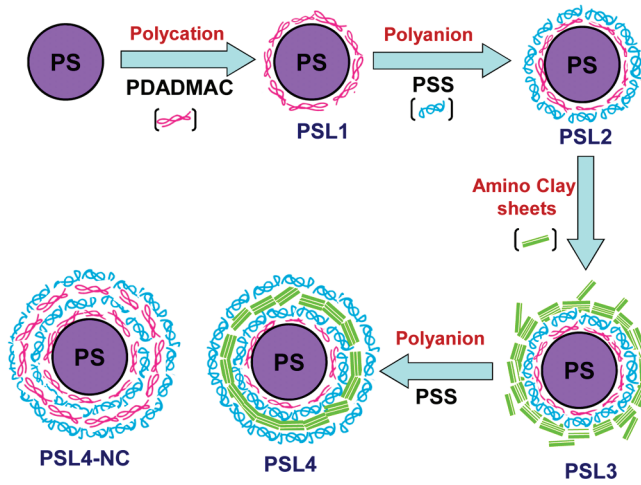

Scheme 1. Scheme showing the formation of PSL4 spheres.

The as-synthesized PS colloids were in the range 680 ± 40 nm in diameter as measured by DLS and scanning electron microscopy (FESEM). The success of the coating of each layer of polyelectrolyte and clay was verified by monitoring the changes in the surface charge using zeta potential measurements at pH 7 (Figure 3a). As expected, the zeta potential for PSL1, PSL2, PSL3, and PSL4 varied between positive and negative values (+40 to −60 mV at pH 7) depending on the charge on the polyelectrolyte or the clay on the outer layer. However, in the case of PSL3, the increase in the positive charge on the surface was minimal (+10 mV) probably due to less charge density on the clay layers compared to the polyelectrolytes at pH 7.

As a next step, we followed the size changes of the spheres brought about by the coating of polyelectrolytes and clay (Figure 3b). From the DLS data, it is evident that each layer of coating of polyelectrolyte increased the thickness of the sphere by 100 nm (for PSL1 and PSL2). The size of PSL3 from DLS suggested an increase in the layer thickness corresponding to the clay coating of around 250 nm. However, the size of PSL3 was found to be unstable over a period of time due to dissociation of clay layers from the surface of the spheres (Figure 3c). In order to stabilize the size of PSL3, it was necessary to protect the clay layers from getting stripped away completely. Therefore, an additional layer of negatively charged PSS over the positively charged clay layers was essential to reduce the stripping of clay. The significant increase in the size stability of PSL4 is shown in Figure 3d. Moreover, it should be mentioned that the thickness of layers obtained from DLS is from the change in hydrodynamic radius of the PS spheres on coating with polyelectrolytes and clay

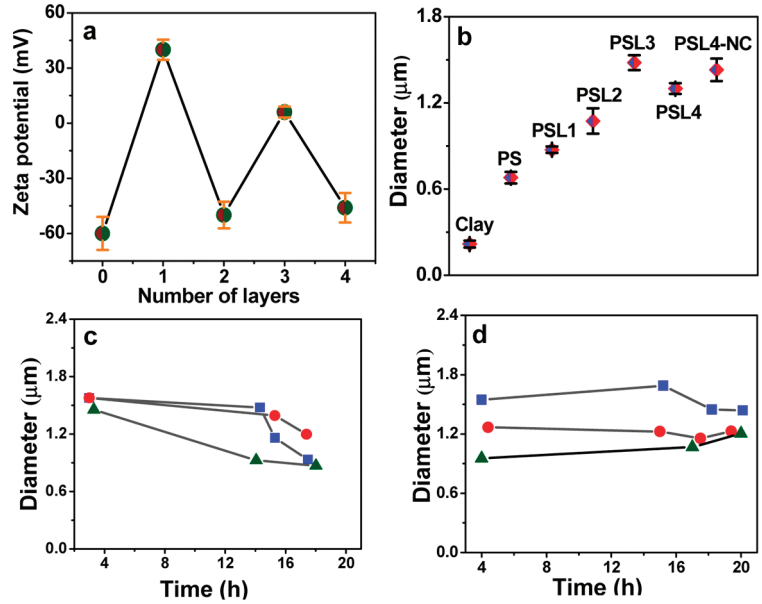

Figure 3. Monitoring coatings: (a) zeta potential variation with number of layers on PS; (b) hydrodynamic diameter of aminoclay, PS, PSL1, PSL2, PSL3, PSL4, and PSL4-NC; (c) variation of hydrodynamic diameter of PSL3 with time; (d) variation of hydrodynamic diameter of PSL4 with time. For (c) and (d) diameter measured at pH 4 (blue squares), pH 7 (red circles), and pH 9 (olive triangles).

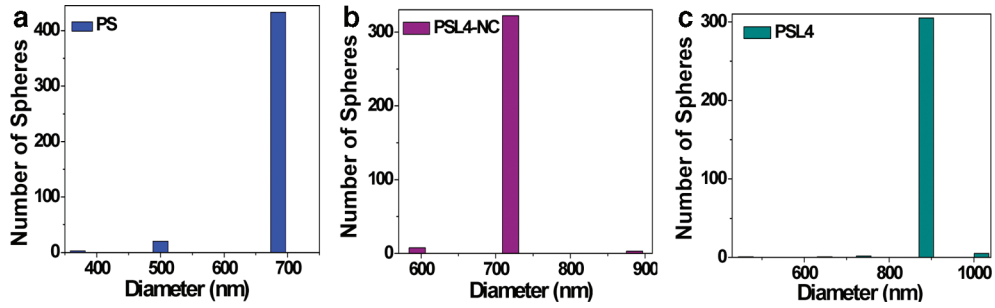

Figure 4. Statistical sizing using FESEM images: (a) PS, (b) PSL4-NC, (c) PSL4.

layers and can be influenced by the density of charges on the surface. We have also calculated the size increase due to polyelectrolytes and the clay layer coating from the FESEM images of the spheres in a dried state.

The average sizes calculated from FESEM for PS, PSL4, and PSL4-NC spheres (Figure S1) were found to be 685, 890 and 720 nm, respectively (Figure 4). From the size differences between PS and PSL4-NC, it is estimated that the thickness of 4 layers of polyelectrolyte coating is around 18 nm, which is nearly the same as the thickness reported (~4 nm per layer) in the literature.[20,48] The thickness due to clay coating is around 89 nm (measured from the size difference between PS and PSL4 spheres, giving room for the three polyelectrolyte layer thickness, ~14 nm). This suggests that the thickness associated with the clay coating is roughly equivalent to 64 layers of clay considering the d_{001} spacing of 1.4 nm for the aminoclay in the XRD pattern (Figure 5e). The higher magnification FESEM (Figure 5a) and TEM image of PSL4 (Figure 5b) further shows increased surface roughness as compared to PS (Figures 5c) due to the presence of the inorganic clay structure. Energy dispersive X-ray analysis on PSL4 showed the presence of Mg and Si originating from the clay sheets (Figure 5d). The broad, low-angle peak appearing in the powder XRD pattern of PSL4 (Figure 5e) was due to the reflection from (001) planes of clay resulting from the turbo static stacking of the layers.

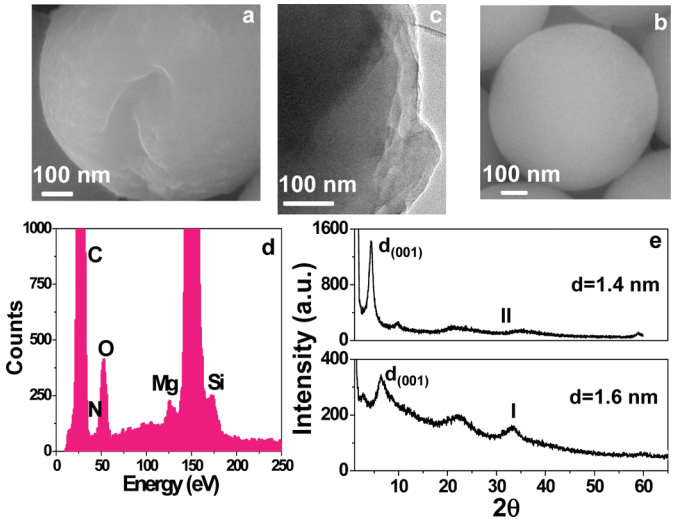

Figure 5. Characterization of PSL4: (a) high-resolution FESEM image of PSL4, (b) TEM image of PSL4, (c) high-resolution FESEM image of PS, (d) EDAX plot of PSL4, (e) XRD pattern of (II) native clay and (I) PSL4.

The dynamic role played by clay layers in PSL4 spheres was studied in its colloidal state using DLS technique. The high dispersibility (zeta potential −40 mV at pH 7) and the monodispersity of PSL4 allowed the study of volume changes more easily using DLS. DLS technique has been commonly used in the past to study colloidal systems of size less than 5 μm.[64−67] The hydrodynamic radius of PSL4 was monitored over a wide range of pH from 3 to 12, and the data are presented in Figure 6a. It can be observed that the size of PSL4 increased steadily from 1 to 1.62 μm as the pH was decreased from 9 to 4. A slight increase in size at pH values beyond 10 was also observed. Interestingly, the size change was reversible over the pH range from 4 to 9. The absence of pH-dependent size oscillation in the case of PS and PSL4-NC spheres highlights the importance of clay in PSL4. The oscillation of size of PSL4 was repeatable for several cycles of pH changes between 4 and 9 (Figure 6b) and is significant that it occurs in a physiologically relevant pH range. The size change was also observed directly under a confocal microscope with the aid of rhodamine 6G labeled PSL4 (Figure S2). The sizes of a number of PSL4 spheres were measured at pH values 4, 7, and 9, and a plot of the histogram is shown in Figure 7a. The sizes of the PSL4-NC spheres at different pH were also measured for comparison (Figures 7b). The histogram clearly shows a shift in the size distribution maxima for PSL4 (compared to PSL4-NC) toward larger sizes with decreasing pH. Further, the shift was reversible between pH 4 and 9 (Figure S3), a trend that was similar to the one observed in DLS measurement.

The unique property of size oscillation of PSL4 is a phenomenon arising out of the confinement of clay layers (or bundle of layers) in the polyelectrolyte matrix. It is important to note that the free aminoclay in water becomes exfoliated more and more as the pH is reduced. However, when the clay is confined in a smaller volume, the extent of exfoliation is greatly reduced. Unlike free aminoclay, the clay in PSL4 is sandwiched between polyelectrolyte layers, which physically entrap the clay layers and prevents their free exfoliation. Rather, it swells with a decrease in pH by the inclusion of water

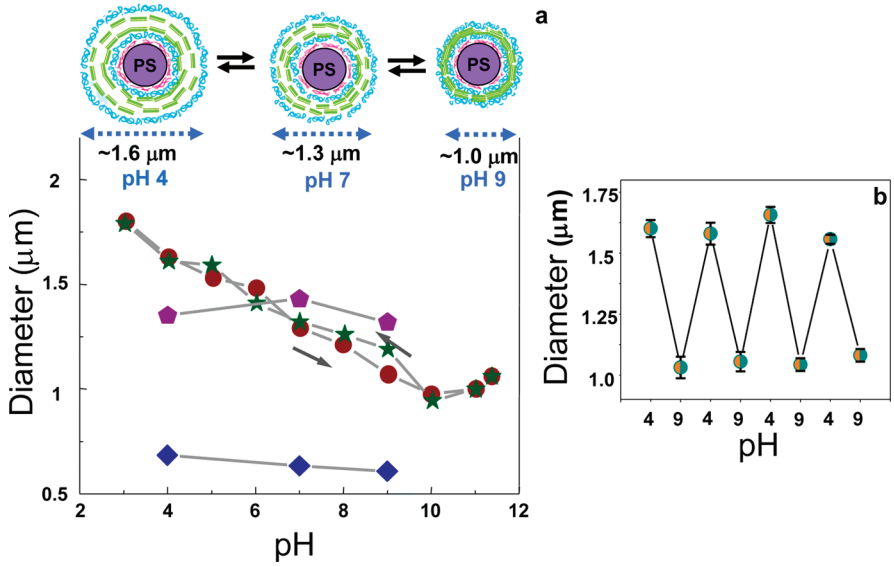

Figure 6. Breathing behavior of PSL4. (a) Size variation of PSL4 with increasing pH (olive stars) and with decreasing pH (wine circles), of PSL4-NC (violet pentagons), of PS (blue diamonds). Cartoon in inset shows the size variation of PSL4, due to swelling/deswelling of clay in the third layer, with respect to pH. (b) Reversible size change, for four cycles.

molecules around the protonated amine groups (Scheme 2). Such swelling effects are observed in the polyelectrolytes only at a very low pH (<2.5) or at a very high pH (>11.5) and are not stable for a longer period.[68,69]

The size oscillation resulting from the degree of protonation of amino groups present in the clay is effectively used to demonstrate a pH-dependent release of oppositely charged molecules. In an acidic pH, the clay sheets inside the PSL4 would be positively charged and can intercalate negatively charged molecules.[44] To demonstrate the application of PSL4 for small-molecule delivery, a model drug, Ibuprofen (pK_a = 4.4), which is commonly used in the treatment of arthritis, primary dysmenorrhea, fever, *etc.*, was chosen. After an equilibration time of 10 h, at pH 6.3, the amount of ibuprofen adsorbed per gram of PSL4 was around 3 mg (Figure S4). The release properties of the drug over PSL4 was monitored for 1 h at pH 4, 7, and 9.8, and the results are given in the bar diagram in Figure 8a. The release behavior of the drug over PSL4-NC was also studied for comparison. From Figure 8a, it is clear that nearly 40% of the drug was released at pH 7, a slightly higher pH than the drug loading pH, 6.3. As the pH was increased to 9.8, the release was about 90%. However, at pH 4, the release of the drug was around 55%, significantly lower than the release at pH 9.8, but still higher than the release at pH 7. On the other hand, the sample without the clay layer (PSL4-NC) did not show any appreciable variation over the entire pH range studied. At high pH, the extent of protonation in aminoclay is low, and therefore, the electrostatic interaction between the negatively charged ibuprofen molecules and the clay layers in PSL4 will be very much reduced. The repulsion

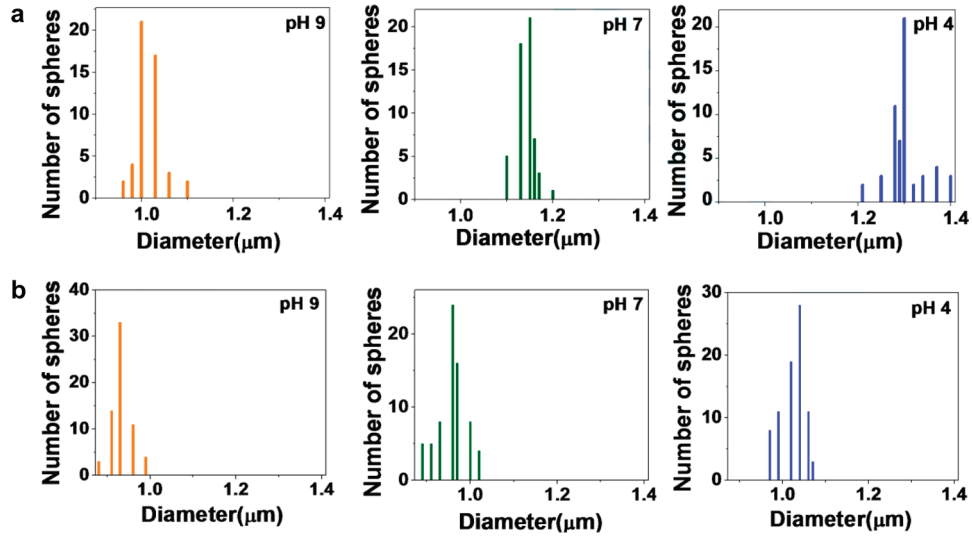

Figure 7. Statistical sizing at different pH using confocal images: (a) PSL4 and (b) PSL4-NC.

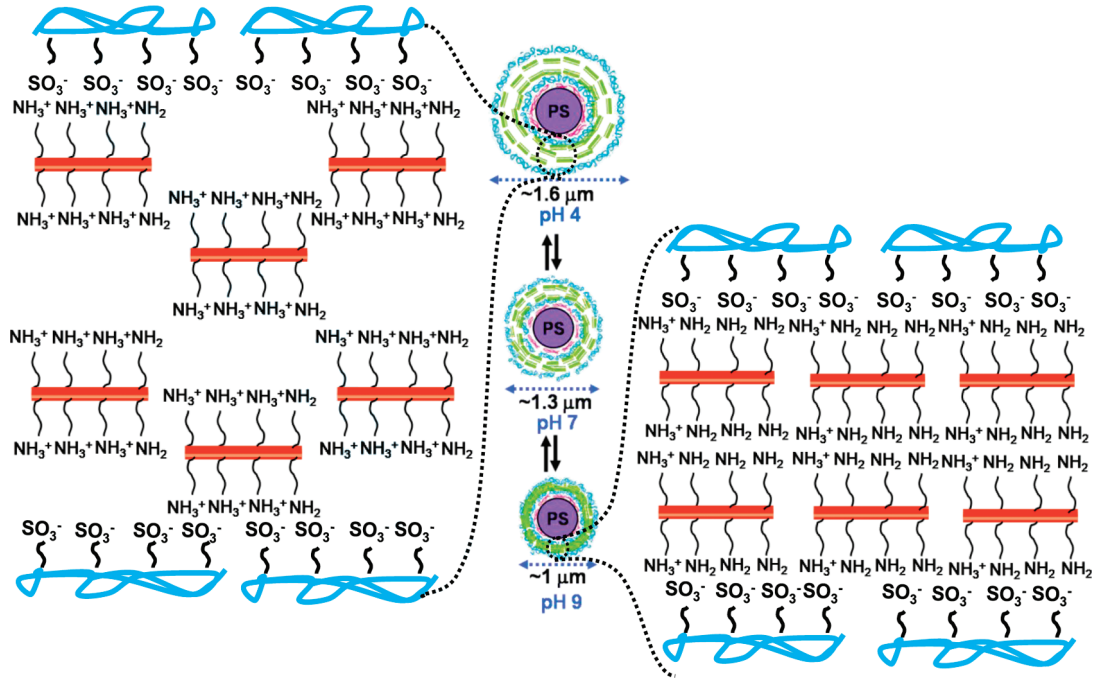

Scheme 2. Schematic showing swelling and deswelling of aminoclay layers inside the polyelectrolyte matrix, which results in size changes of PSL4 with pH (water molecules surrounding protonated amine groups are not shown for clarity).

between the negatively charged ibuprofen molecules combined with the shrinking of spheres contributes to the higher release at pH 9.8. At neutral pH, the strong electrostatic interaction between the protonated aminoclay and the negatively charged ibuprofen reduces the release level. As the pH goes below the pK_a value of the ibuprofen (pK_a = 4.4), more amino groups in the clay layers are getting protonated, whereas the drug molecules are becoming neutral. This again reduces the electrostatic interaction between the clay layers and the drug molecules and hence enhances the drug release.[70] This release behavior is different from the release of ibuprofen from the mesoporous materials, where the rate of release was increased with increase in pH in the first hour due to increased solubility of the drug molecule.[71] However, when the dye eosin (pK_{a1} = 3.25)[72] was used to study the release properties of PSL4 spheres, it shows a different behavior (Figure 8b). About 70% of the dye was released even at pH 7, which was more or less equal to the amount released at higher pH, 9.8 (~75%). Reducing the pH of the medium to 4 markedly reduces the release of the eosin molecules to 27%, a distinct deviation from the ibuprofen behavior. At pH 4, the dye molecules are still negatively charged[72] and will have strong binding to the highly protonated clay layer, which therefore reduces the dye release to the observed lower level.

Our efforts to obtain hollow capsules by dissolving the PS core of PSL4 in tetrahydrofuran failed due to the disruption of the fragile walls of the spheres. Fortification of the walls by increasing the number of layers to 13 (PSL13) with the clay layer in the middle (7th layer) still results in the reversible volume oscillation with respect to pH (Figure 9a). However, dissolution of polystyrene spheres once again leads to their collapse, probably due to osmotic swelling as the dissolved PS leaves large polymer fragments that cannot permeate out through the polyelectrolyte layers.[20] We therefore made composite spheres similar to PSL13 using $CaCO_3$ spheres as cores. It was possible to successfully pro-

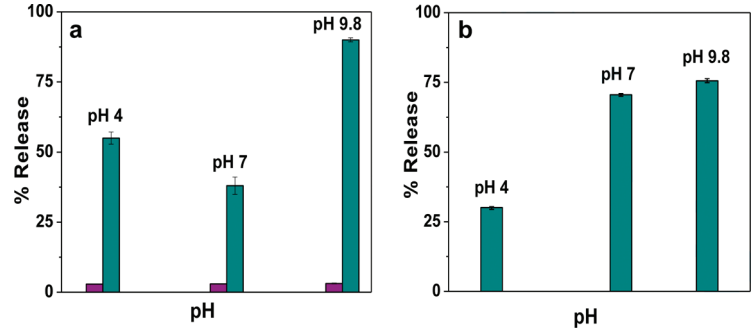

Figure 8. Release behavior of PSL4 at different pH observed for 1 h: (a) release of loaded drug, ibuprofen; (b) release of dye, eosin. Cyan bar is for PSL4 and purple bar is for PSL4-NC.

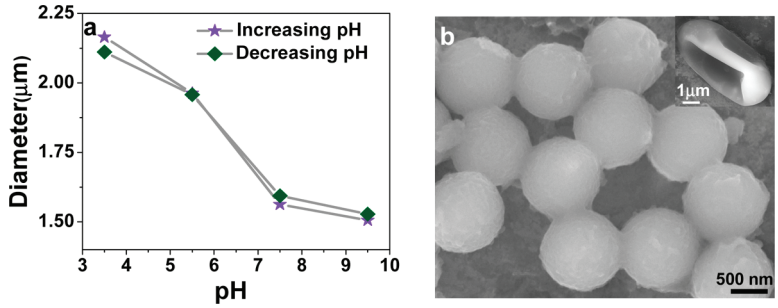

Figure 9. Capsule preparation: (a) size variation of PSL13 spheres with respect to pH; (b) capsules prepared from CaL13 (inset shows a single buckled capsule).

duce hollow capsules of polyelectrolyte−clay composite by dissolving the $CaCO_3$ core using ethylenediaminetetraacetic acid (EDTA) (see Experimental Section) (Figure 9b). The absence of Ca in the EDX analysis (Figure S5) confirms the complete removal of $CaCO_3$, leaving the hollow spheres intact due to the presence of inorganic clay component. This is in contrast to the collapsed spheres usually obtained for polyelectrolyte capsules. The buckled morphology (shown in the inset of Figure 9b) templated from a very large calcium carbonate sphere reveals the hollow nature of the spheres after removal of the template.

CONCLUSIONS

In conclusion, we have demonstrated for the first time the utility of organoclays to form pH-responsive spheres. The composites were shown to reversibly expand and shrink in size by 1.6 times over a wide range of pH (4 to 9) due to the protonation of amino groups in the clay layers. This unique behavior of composite spheres was used to demonstrate pH-dependent release of a negatively charged drug molecule like ibuprofen in the physiologically relevant pH range, i.e., 4.5 to 7.5. It was also shown that the composite sphere could be successfully used to adsorb eosin quite effectively. The future development of this material could involve changing the hydrophilicity of the clay layers. By increasing the length of the alkylamino pendent groups, one can load both hydrophobic and hydrophilic drugs. Furthermore, the hollow capsules prepared after core dissolution can have special advantages over the existing microcapsules, as they can be loaded with two different kinds of guest molecules, reactants, or drugs for dual delivery applications.

MATERIALS AND METHODS

Materials. Styrene monomers (Aldrich), $K_2S_2O_8$ (Merck, India), PDADMAC (Aldrich, M_w < 200 000) and PSS (Aldrich, M_w 70 000), $MgCl_2$ (Merck, India), 3-aminopropyltriethoxysilane (Aldrich), ethanol (HPLC grade), tetrahydrofuran, ethylenediaminetetraacetic acid, $CaCl_2 \cdot 2H_2O$ (Merck, India), and Na_2CO_3 (Ranbaxy, India) were used.

Synthesis of PS. Monodisperse polystyrene spheres were synthesized as described elsewhere.[42] A 3.92 mL amount of styrene monomer was added to 50 mL of water, maintained at 70 °C, followed by slow addition of an aqueous solution of $K_2S_2O_8$ (0.082 g in 3.57 mL of water), with continuous stirring in nitrogen atmosphere. The resulting solution was stirred for 24 h. Finally, the emulsion was naturally cooled to ambient temperature and filtered to get PS spheres.

Synthesis of Clay. An aminopropyl-functionalized magnesium (organo)phyllosilicate clay was synthesized[43] at room temperature by dropwise addition of 3-aminopropyltriethoxysilane (1.3 mL, 5.85 mmol) to an ethanol solution of magnesium chloride (0.84 g, 3.62 mmol in 20 g of ethanol). The white slurry obtained after 5 min was stirred overnight, and the precipitate was isolated by centrifugation, washed with ethanol (50 mL), and dried at 40 °C.

Fabrication of Composite PSL4 and PSL13. Polyelectrolytes and clay were coated on polystyrene colloids (~680 nm) using a layer-by-layer method. For PSL4 the order of coating was PDADMAC, PSS, clay, and PSS, and for PSL13 the order was $(PDADMAC/PSS)_3$, clay, and $(PSS/PDADMAC)_3$. The concentration of the polyelectrolytes and clay solutions used was 2 mg/mL. The adsorption of polyelectrolytes was carried out in 0.5 M NaCl solution for 20 min followed by centrifugation at 13 500 rpm for 15 min. This was followed by three cycles of centrifugation/washing in water. The clay coating was done in 0.5 M NaCl solution for 1 h followed by washing with water.

DLS Size and Zeta Potential Measurements. The hydrodynamic diameter and the zeta potential measurements at different pH were carried out using Zetasizer Nano ZS (Malvern Instruments). The temperature for the measurement was kept at 25 °C. The concentration of the samples was 0.03% w/v. The pH of the solutions was adjusted using 0.5 M aqueous HCl/NaOH solutions.

Confocal Imaging. Confocal laser scanning fluorescence microcopy of PSL4 was done on a Zeiss LSM 510 Meta (Carl Zeiss). The instrument was equipped with 100× oil immersion objective with numerical aperture of 1.3. Dilute solutions of PSL4 were maintained at the desired pH using 0.5 M aqueous HCl/NaOH solutions. To 100 μL of these solutions was added 2 μL of 0.1% w/v rhodamine 6G solution. Samples were excited using a He−Ne laser, wavelength 543 nm. For precise size measurements of spheres at different pH, fluorescence profiling was done along a diametric line. Size of the sphere was calculated by taking the difference between the intensity minima positions at the two ends of this line.

Adsorption and Release of Ibuprofen/Eosin. The ibuprofen (or eosin) adsorption and release studies were done by monitoring photoluminescence (PL) intensity at an emission wavelength of 303 nm (or 538 nm) (λ_{ex} = 219 nm for ibuprofen and 515 nm for eosin). To load ibuprofen drug, 1.7 mg of PSL4 was dispersed in 1 mL of aqueous solution containing 63 μg of the drug. This was allowed to equilibrate for 10 h at pH 6.3 followed by syringe filtration (Puradisc 4, Whatman). The amount of drug adsorbed at pH 9 was calculated using a calibration plot (PL intensity vs drug concentration). This pH was chosen to avoid the experimental error likely to occur in the measurement of PL intensity due to large fluctuations in dissociation near the pK_a value of the drug/dye. Finally the drug or dye loaded PSL4 (1.7 mg) was dispersed

in Milli-Q water (1 mL) at different pH (4, 7, 9) for 1 h and was filtered. On the basis of the PL intensity of the filtrate measured at pH 9 the amount of released drug or dye was calculated.

Capsule Preparation. The capsules were prepared from the polyelectrolyte- and clay-coated $CaCO_3$ spheres by dissolving the template. The $CaCO_3$ spheres, 3−4 μm in size, were synthesized as described elsewhere.[73] These spheres were coated with multiple layers of polyelectrolytes keeping the clay layer in the middle in the following order: $(PSS/PDADMAC)_3$−PSS−clay−$(PSS/PDADMAC)_2$−PSS. To dissolve the $CaCO_3$ core of these polyelectrolyte/clay-coated spheres, 10 mg of the sample was added to 1 mL of 0.2 M EDTA solution. The solution was stirred for 30 min and then centrifuged at 2000 rpm for 5 min. The solid precipitate was dispersed in Milli-Q water and centrifuged. Washing with water was done three times.

Acknowledgment. The authors are thankful to Prof. C. N. R. Rao, FRS, for the kind support and encouragement. We thank Dr. Rajesh Ganapathi (ICMS, JNCASR) for the useful discussions on DLS. The authors thank Mrs. B. S. Suma (MBGU, JNCASR) for the confocal measurements and Mrs. N. R. Selvi (CPMU, JNCASR) for FESEM measurements.

Supporting Information Available: FESEM image of PS, PSL4-NC, and PSL4, confocal images and fluorescence profiling for size measurement of PSL4 at different pH, statistical sizing of PSL4 for two cycles of pH change, adsorption of drug, and EDX for hollow sphere. This material is available free of charge *via* the Internet at http://pubs.acs.org.

REFERENCES AND NOTES

1. Stuart, M. A. C.; Huck, W. T. S.; Genzer, J.; Müller, M.; Ober, C.; Stamm, M.; Sukhorukov, G. B.; Szleifer, I.; Tsukruk, V. V.; Urban, M.; Winnik, F.; Zauscher, S.; Luzinov, I.; Minko, S. Emerging Applications of Stumuli-Responsive Polymeric Materials. *Nat. Mater.* **2010**, *9*, 101–113.
2. Xia, F.; Jiang, L. Bio-Inspired, Smart, Multiscale Interfacial Materials. *Adv. Mater.* **2008**, *20*, 2842–2858.
3. Lu, Y.; Liu, J. Smart Nanomaterials Inspired by Biology: Dynamic Assembly of Error-Free Nanomaterials in Response to Multiple Chemical and Biological Stimuli. *Acc. Chem. Res.* **2007**, *40*, 315–323.
4. Luzinova, I.; Minko, S.; Tsukruk, V. V. Adaptive and Responsive Surfaces through Controlled Reorganization of Interfacial Polymer Layers. *Prog. Polym. Sci.* **2004**, *29*, 635–698.
5. Dai, C. D.; Eakins, D. E.; Thadhani, N. N. Dynamic Densification Behavior of Nanoiron Powders Under Shock Compression. *J. Appl. Phys.* **2008**, *103*, 093503.
6. Soppimath, K. S.; Liu, L. H.; Seow, W. Y.; Liu, S. Q.; Powell, R.; Chan, P.; Yang, Y. Multifunctional Core/Shell Nanoparticles Self-Assembled from pH-Induced Thermosensitive Polymers for Targeted Intracellular Anticancer Drug Delivery. *Adv. Funct. Mater.* **2007**, *17*, 355–362.
7. Tan, W. S.; Cohen, R. E.; Rubner, M. F.; Sukhishvili, S. A. Temperature-Induced, Reversible Swelling Transitions in Multilayers of a Cationic Triblock Copolymer and a Polyacid. *Macromolecules* **2010**, *43*, 1950–1957.
8. Yameen, B.; Ali, M.; Neumann, R.; Ensinger, W.; Knoll, W.; Azzaroni, O. Single Conical Nanopores Displaying pH-Tunable Rectifying Characteristics. Manipulating Ionic Transport with Zwitterionic Polymer Brushes. *J. Am. Chem. Soc.* **2009**, *131*, 2070–2071.
9. Sukhorukov, G. B.; Antipov, A. A.; Voigt, A.; Donath, E.; Möhwald, H. pH-Controlled Macromolecule Encapsulation in and Release from Polyelectrolyte Multilayer Nanocapsules. *Macromol. Rapid Commun.* **2001**, *22*, 44–46.
10. Garnweitner, G.; Smarsly, B.; Assink, R.; Ruland, W.; Bond, E.; Brinker, C. J. Self-Assembly of an Environmentally Responsive Polymer/Silica Nanocomposite. *J. Am. Chem. Soc.* **2003**, *125*, 5626–5627.
11. Mauser, T.; Déjugnat, C.; Sukhorukov, G. B. Balance of Hydrophobic and Electrostatic Forces in the pH Response of Weak Polyelectrolyte Capsules. *J. Phys. Chem. B* **2006**, *110*, 20246–20253.
12. Mauser, T.; Déjugnat, C.; Sukhorukov, G. B. Reversible pH-Dependent Properties of Multilayer Microcapsules Made of Weak Polyelectrolytes. *Macromol. Rapid Commun.* **2004**, *25*, 1781–1785.
13. Kwon, I. C.; Bae, Y. H.; Kim, S. W. Electrically Erodable Polymer Gel for Controlled Release of Drugs. *Nature* **1991**, *354*, 291–293.
14. Cai, K.; Luo, Z.; Hu, Y.; Chen, X.; Liao, Y.; Yang, L. Linhong Magnetically Triggered Reversible Controlled Drug Delivery from Microfabricated Polymeric Multireservoir Devices. *Adv. Mater.* **2009**, *21*, 4045–4049.
15. Mai, Y.; Dong, W.; Hempenius, M. A.; Möhwald, H.; Vancso, G. J. Redox-Controlled Molecular Permeability of Composite-Wall Microcapsules. *Nat. Mater.* **2006**, *5*, 724–729.
16. Park, J. M.; Aoyama, S.; Zhang, W.; Nakatsuji, Y.; Ikeda, I. Photodimerisation of a Styrylpyrazine Amphiphile Suppresses the Release of Glucose Entrapped in its Mixed Vesicle with DPPC. *Chem. Commun.* **2000**, 231–232.
17. Liu, N.; Chen, Z.; Dunphy, D. R.; Jiang, Y. B.; Assink, R. A.; Brinker, C. J. Photoresponsive Nanocomposite Formed by Self-Asssembly of an Azobenzene-Modified Silane. *Angew. Chem., Int. Ed.* **2003**, *42*, 1731–1734.
18. Ishihara, K.; Muramoto, N.; Shinohara, I. Controlled Release of Organic Substances Using Polymer Membranes with Responsive Function for Amino Compounds. *J. Appl. Polym. Sci.* **1984**, *29*, 211–217.
19. Ibarz, G.; Dähne, L.; Donath, E.; Möhwald, H. Smart Micro- and Nanocontainers for Storage, Transport, and Release. *Adv. Mater.* **2001**, *13*, 1324–1327.
20. Peyratout, C. S.; Dähne, L. Tailor-Made Polyelectrolyte Microcapsules: From Multilayers to Smart Containers. *Angew. Chem., Int. Ed.* **2004**, *43*, 3762–3783.
21. Yu, S.; Azzam, T.; Rouiller, I.; Eisenberg, A. "Breathing" Vesicles. *J. Am. Chem. Soc.* **2009**, *131*, 10557–10566.
22. Sandström, M. C.; Ickenstein, L. M.; Mayer, L. D.; Edwards, K. Effects of Lipid Segregation and Lysolipid Dissociation on Drug Release from Thermosensitive Liposomes. *J. Controlled Release* **2005**, *107*, 131–148.
23. Kang, Y.; Walish, J. J.; Gorishnyy, T.; Thomas, E. L. Broad-Wavelength-Range Chemically Tunable Block-Copolymer Photonic Gels. *Nat. Mater.* **2007**, *6*, 957–960.
24. Feuchtwanger, J.; Asua, E.; García-Arribas, A.; Etxebarria, V.; Barandiaran, J. M. Ferromagnetic Shape Memory Alloys for Positioning with Nanometric Resolution. *Appl. Phys. Lett.* **2009**, *95*, 054102.
25. Cohen, R. E. Origin of Ferroelectricity in Perovskite Oxides. *Nature* **1992**, *358*, 136–138.
26. Jaffe, B.; Cook, W. R.; Jaffe, H. *Piezoelectric Ceramics*; Academic: New York, 1971.
27. Ehre, D.; Lyahovitskaya, V.; Tagantsev, A.; Lubomirsky, I. Amorphous Piezo and Pyroelectric Phases of $BaZrO_3$ and $SrTiO_3$. *Adv. Mater.* **2007**, *19*, 1515–1517.
28. Nunes, S. C.; Bermudez, V. D. Z.; Silva, M. M.; Smith, M. J.; Ostrovskii, D.; Ferreira, R. A. S.; Carlos, L. D.; Rocha, J.; Gonçalves, A.; Fortunato, E. Sol-Gel-Derived Potassium-Based di-Ureasils for "Smart Windows". *J. Mater. Chem.* **2007**, *17*, 4239–4248.
29. Kickelbick, G. *Hybrid Materials: Synthesis, Characterization and Application*; Wiley-VCH: Weinheim, Germany, 2007; pp 7−9.
30. Capadona, J. R.; Shanmuganathan, K.; Tyler, D. J.; Rowan, S. J.; Weder, C. Stimuli-Responsive Polymer Nanocomposites Inspired by the Sea Cucumber Dermis. *Science* **2008**, *319*, 1370–1374.
31. Katagiri, K.; Nakamura, M.; Koumoto, K. Magnetoresponsive Smart Capsules Formed with Polyelectrolytes, Lipid Bilayers and Magnetic Nanoparticles. *ACS Appl. Mater. Interfaces* **2010**, *2*, 768−773.
32. Schmidt, D. J.; Cebeci, F. C.; Kalcioglu, Z. I.; Wyman, S. G.; Ortiz, C.; Vliet, K. J. V.; Hammond, P. T. Electrochemically Controlled Swelling and Mechanical Properties of a Polymer Nanocomposite. *ACS Nano* **2009**, *3*, 2207–2216.
33. Motornov, M.; Zhou, J.; Pita, M.; Gopishetty, V.; Tokarev, I.;

Katz, E.; Minko, S. "Chemical Transformers" from Nanoparticle Ensembles Operated with Logic. *Nano Lett.* **2008**, *8*, 2993–2997.
34. Riskin, M.; Basnar, B.; Huang, Y.; Willner, I. Magnetoswitchable Charge Transport and Bioelectrocatalysis Using Maghemite-Au Core-Shell Nanoparticle/Polyaniline Composites. *Adv. Mater.* **2007**, *19*, 2691–2695.
35. Bédard, M.; Skirtach, A. G.; Sukhorukov, G. B. Optically Driven Encapsulation Using Novel Polymeric Hollow Shells Containing an Azobenzene Polymer. *Macromol. Rapid Commun.* **2007**, *28*, 1517–1521.
36. Geest, B. G. D.; Skirtach, A. G.; Mamedov, A. A.; Antipov, A. A.; Kotov, N. A.; Smedt, S. C. D.; Sukhorukov, G. B. Ultrasound-Triggered Release from Multilayered Capsules. *Small* **2007**, *3*, 804–808.
37. Liu, N.; Yu, K.; Smarsly, B.; Dunphy, D. R.; Jiang, Y.-B.; Brinker, C. J. Self-Directed Assembly of Photoactive Hybrid Silicates Derived from an Azobenzene-Bridged Silsesquioxane. *J. Am. Chem. Soc.* **2002**, *124*, 14540–14541.
38. Muthusamy, E.; Walsh, D.; Mann, S. Morphosynthesis of Organoclay Microspheres with Sponge-Like or Hollow Interiors. *Adv. Mater.* **2002**, *14*, 969–972.
39. Putlitz, B. Z.; Landfester, K.; Fischer, H.; Antonietti, M. The Generation of "Armored Latexes" and Hollow Inorganic Shells Made of Clay Sheets by Templating Cationic Miniemulsions and Latexes. *Adv. Mater.* **2001**, *13*, 500–503.
40. Bourlinos, A. B.; Karakassides, M. A.; Petridis, D. Synthesis and Characterization of Hollow Clay Microspheres through a Resin Template Approach. *Chem. Commun.* **2001**, 1518–1519.
41. Caruso, R. A.; Susha, A.; Caruso, F. Multilayered Titania, Silica, and Laponite Nanoparticle Coatings on Polystyrene Colloidal Templates and Resulting Inorganic Hollow Spheres. *Chem. Mater.* **2001**, *13*, 400–409.
42. Furusawa, K.; Norde, W.; Lyklema, A. Method for Preparing Surfactant-Free Polystyrene Latices of High Surface Charge. *J. Kolloid-ZZ Polym.* **1972**, *250*, 908–909.
43. Patil, A. J.; Muthusamy, E.; Mann, S. Synthesis and Self-Assembly of Organoclay-Wrapped Biomolecules. *Angew. Chem., Int. Ed.* **2004**, *43*, 4928–4933.
44. Datta, K. K. R.; Eswaramoorthy, M.; Rao, C. N. R. Water-Solubilized Aminoclay-Metal Nanoparticle Composites and their Novel Properties. *J. Mater. Chem.* **2007**, *17*, 613–615.
45. Che, S.; Garcia-Bennett, A. E.; Yokoi, T.; Sakamoto, K.; Kunieda, H.; Terasaki, O.; Tatsumi, T. A Novel Anionic Surfactant Templating Route for Synthesizing Mesoporous Silica with Unique Structure. *Nat. Mater.* **2003**, *2*, 801–805.
46. Decher, G. Fuzzy Nanoassemblies: Toward Layered Polymeric Multicomposites. *Science* **1997**, *277*, 1232–1237.
47. Kleinfeld, E. R.; Ferguson, G. S. Stepwise Formation of Multilayered Nanostructural Films from Macromolecular Precursors. *Science* **1994**, *265*, 370–373.
48. Kozlovskaya, V.; Kharlampieva, E.; Erelb, I.; Sukhishvili, S. A. Multilayer-Derived, Ultrathin, Stimuli-Responsive Hydrogels. *Soft Matter* **2009**, *5*, 4077–4087.
49. Srivastava, S.; Kotov, N. A. Composite Layer-by-Layer (LBL) Assembly with Inorganic Nanoparticles and Nanowires. *Acc. Chem. Res.* **2008**, *41*, 1831–1841.
50. Hammond, P. T. Form and Function in Multilayer Assembly: New Applications at Nanoscale. *Adv. Mater.* **2004**, *16*, 1271–1293.
51. Kotov, N. A.; Dekany, I.; Fendler, J. H. Layer-by-Layer Self-Assembly of Polyelectrolyte-Semiconductor Nanoparticle Composite Films. *J. Phys. Chem.* **1995**, *99*, 13065–13069.
52. Mamedov, A. A.; Kotov, N. A.; Prato, M.; Guldi, D. M.; Wicksted, J. P.; Hirsch, A. Molecular Design of Strong Single-Wall Carbon Nanotube/Polyelectrolyte Multilayer Composites. *Nat. Mater.* **2002**, *1*, 190–194.
53. Jiang, C.; Ko, H.; Tsukruk, V. V. Strain-Sensitive Raman Modes of Carbon Nanotubes in Deflecting Freely Suspended Nanomembranes. *Adv. Mater.* **2005**, *17*, 2127–2131.
54. Kleinfeld, E. R.; Ferguson, G. S. Healing of Defects in the Stepwise Formation of Polymer/Silicate Multilayer Films. *Chem. Mater.* **1996**, *8*, 1575–1578.
55. Kleinfeld, E. R.; Ferguson, G. S. Rapid, Reversible Sorption of Water from the Vapor by a Multilayered Composite Film: A Nanostructured Humidity Sensor. *Chem. Mater.* **1995**, *7*, 2327–2331.
56. Lvov, Y.; Decher, G.; Sukhorukov, G. Assembly of Thin Films by Means of Successive Deposition of Alternate Layers of DNA and poly(allylamine). *Macromolecules* **1993**, *26*, 5396–5399.
57. Hong, J. D.; Lowack, K.; Schmitt, J.; Decher, G. Layer-by-Layer Deposited Multilayer Assemblies of Polyelectrolytes and Proteins: from Ultrathin Films to Protein Arrays. *Prog. Colloid Polym. Sci.* **1993**, *93*, 98–102.
58. Lvov, Y.; Ariga, K.; Kunitake, T. Layer-by-Layer Assembly of Alternate Protein/Polyion Ultrathin Films. *Chem. Lett.* **1994**, *12*, 2323–2326.
59. Yoo, P. J.; Nam, K. T.; Qi, J.; Lee, S. K.; Park, J.; Belcher, A. M.; Hammond, P. T. Spontaneous Assembly of Viruses on Multilayered Polymer Surfaces. *Nat. Mater.* **2006**, *5*, 234–240.
60. Cassier, T.; Sinner, A.; Offenhauser, A.; Mohwald, H. Homogeneity, Electrical Resistivity and Lateral Diffusion of Lipid Bilayers Coupled to Polyelectrolyte Multilayers. *Colloids Surf. B* **1999**, *15*, 215–225.
61. Geest, B. G. D.; Sanders, N. N.; Sukhorukov, G. B.; Demeestera, J.; Smedt, S. C. D. Release Mechanisms for Polyelectrolyte Capsules. *Chem. Soc. Rev.* **2007**, *36*, 636–649.
62. Geest, B. G. D.; Koker, S. D.; Sukhorukov, G. B.; Kreft, O.; Parak, W. J.; Skirtach, A. G.; Demeester, J.; Smedt, S. C. D.; Hennink, W. E. Polyelectrolyte Microcapsules for Biomedical Applications. *Soft Matter* **2009**, *5*, 282–291.
63. Angelatos, A. S.; Katagiri, K.; Caruso, F. Bioinspired Colloidal Systems *via* Layer-by-Layer Assembly. *Soft Matter* **2006**, *2*, 18–23.
64. Nalluri, S. K. M.; Ravoo, B. J. Light-Responsive Molecular Recognition and Adhesion of Vesicles. *Angew. Chem., Int. Ed.* **2010**, *49*, DOI: 10.1002/anie.201001442.
65. Yin, J.; Dupin, D.; Li, J.; Armes, S. P.; Liu, S. pH-Induced Deswelling Kinetics of Sterically Stabilized Poly(2-vinylpyridine) Microgels Probed by Stopped-Flow Light Scattering. *Langmuir* **2008**, *24*, 9334–9340.
66. Dupin, D.; Rosselgong, J.; Armes, S. P.; Routh, A. Swelling Kinetics for a pH-Induced Latex-to-Microgel Transition. *Langmuir* **2007**, *23*, 4035–4041.
67. Dupin, D.; Fujii, S.; Armes, S. P.; Reeve, P.; Baxter, S. M. Efficient Synthesis of Sterically Stabilized pH-Responsive Microgels of Controllable Particle Diameter by Emulsion Polymerization. *Langmuir* **2006**, *22*, 3381–3387.
68. Dubas, S. T.; Schlenoff, J. B. Polyelectrolyte Multilayers Containing a Weak Polyacid: Construction and Deconstruction. *Macromolecules* **2001**, *34*, 3736–3740.
69. Déjugnat, C.; Sukhorukov, G. B. pH-Responsive Properties of Hollow Polyelectrolyte Microcapsules Templated on Various Cores. *Langmuir* **2004**, *20*, 7265–7269.
70. Holmström, S. C.; Patil, A. J.; Butler, M.; Mann, S. Influence of Polymer Co-intercalation on Guest Release from Aminopropylfunctionalized Magnesium Phyllosilicate Mesolamellar Nanocomposites. *J. Mater. Chem.* **2007**, *17*, 3894–3900.
71. Lee, K.; Lee, D.; Lee, H.; Kim, C.-K.; Wu, Z.; Lee, K. Comparison of Amine-Functionalized Mesoporous Silica Particles for Ibuprofen Delivery. *Korean J. Chem. Eng.* **2010**, *27*, 1333–1337.
72. Ledlain, P.; Fompeydie, D. Determination of Equilibrium Constants by Derivative Spectrophotometry. Application to the pKas of Eosin. *Anal. Chem.* **1985**, *57*, 2561–2563.
73. Volodkin, D. V.; Petrov, A. I.; Prevot, M.; Sukhorukov, G. B. Matrix Polyelectrolyte Microcapsules: New System for Macromolecule Encapsulation. *Langmuir* **2004**, *20*, 3398–3406.